



LIBRARY Michigan State University

This is to certify that the

thesis entitled

Microstructures of Glacigenic Debris Flow Deposits, Matanuska Glacier, Alaska

presented by

Matthew Scott Lachniet

has been accepted towards fulfillment of the requirements for

Masters degree in Geological Sciences

Major professor

Date May 6, 1997

PLACE IN RETURN BOX to remove this checkout from your record. TO AVOID FINES return on or before date due.

DATE DUE	DATE DUE	DATE DUE

MSU is An Affirmative Action/Equal Opportunity Institution choictelestedus.pm3-p.1

MICROSTRUCTURES OF GLACIGENIC DEBRIS FLOW DEPOSITS, MATANUSKA GLACIER, ALASKA

By

Matthew Scott Lachniet

A THESIS

Submitted to

Michigan State University

in partial fulfillment of the requirements

for the degree of

MASTER OF SCIENCE

Department of Geological Sciences

1997

ABSTRACT

MICROSTRUCTURES OF GLACIGENIC DEBRIS FLOW DEPOSITS, MATANUSKA GLACIER, ALASKA.

By

Matthew Scott Lachniet

The micromorphology of resin-impregnated glacigenic debris flow deposits was analyzed to improve our understanding of their genesis. Debris flows formed at the terminus of the Matanuska Glacier, Alaska, USA, have been classified into four types based primarily on water content and sedimentological characteristics (Lawson, 1979, 1982). Thin sections of debris flow deposits show a variety of micro and mesoscale characteristics that vary according to water content of the source flow. Micro structures present include 1) clast fabrics, 2) laminar structures, 3) plastic structures, 4) brittle structures, and 5) miscellaneous structures. Characterization of these microstructures supports the contention that micromorphological analyses can be used to elucidate debris flow genesis and the conditions of the flow just prior to deposition. Thus, micromorphology may also be useful for differentiating debris flow type in Pleistocene diamicts within the Great Lakes region and other locations.

ACKNOWLEDGEMENTS

I would like to thank my advisor, Dr. Grahame, J. Larson, for two years of excellent advice and encouragement. Thanks also go to the other members of the Matanuska Glacier research group for ideas and comments on this thesis: Dr. Daniel E. Lawson, Dr. Edward B. Evenson, and Dr. Jeffrey C. Strasser. Support for this project was graciously supplied by Dr. Larson at Michigan State University, Dr. Evenson at Lehigh University, and Dr. Lawson at the Cold Regions Research and Engineering Laboratory.

TABLE OF CONTENTS

LIST OF TABLES		V
LIST OF FIGURES		vi
INTRODUCTION		1
SITE DESCRIPTION		3
LITERATURE REVIEW		4
DEBRIS FLOW CLASSIFICATION AT	ΓΗΕ MATANUSKA GLACIER	8
Type flow characteristics		8
Theoretical microstructures of debr	is flow deposits	11
MATERIALS AND METHODS		13
Sampling protocol		13
Sample and thin section preparation	1	14
Terminology		14
RESULTS		18
Moraine site description and sample	e locations	18
Dry-type flow deposit samples	(14, 31, 45, 53, 70)	22
Wet-type flow deposit samples		
DISCUSSION		48
Characteristics of dry-type debris fl	ow deposits	48
	low deposits	
	w deposits	
CONCLUSIONS		54
LIST OF REFERENCES		56

LIST OF TABLES

Table 1 - Characteristics of type debris flows. (After Lawson, 1979)	9
Table 2 - Sample information.	21
Table 3 - Micromorphological characteristics of subaerial glacigenic debris flow	
deposits	51

LIST OF FIGURES

Figure - 1. Map of the Matanuska Glacier and Alaska. (from Lawson, 1979) Figure - 2. Stereograms of flow till fabrics. (From Marcussen, 1975)	5 5
Figure - 3. Mean grain size of debris flows as a function of water content. (From	
Lawson, 1979)	11
Figure - 4. Microstructures of glacial sediments. Adapted from van der Meer	
(1993) by Lachniet and Menzies	17
Figure - 5. Map of the western terminus region. Matanuska Glacier, Alaska	
and a top dry type debris flow unit. Actual size	23
Figure - 7. Detail of top folded sand layer in 14B, of bottom unit, gypsum wedge. Width of view is 27mm.	23
Figure - 8. Detail of 14T, dry type debris flow. Note the fissility planes dipping to the left and the silt clast near the center of photo. Gypsum wedge.	
Width of view is 22mm.	24
Figure - 9. Detail of silt clast in 14T. Note the vertical silt layers. Width of view is 8mm.	24
Figure - 10. Sample 31 thin sections.	26
Figure - 11. Detail of the contact between meltwater silts and the dry type	
debris flow in 31B. The silt layers represent the basal zone of shear.	
Gypsum wedge. Width of view is 22mm	26
Figure - 12. Detail of the basal shear zone from previous figure. Note the	
strain cap and shadow on the small metamorphic clast. Gypsum Wedge.	
Width of view is 8mm.	27
Figure - 13. Detail of deformation bulge in the dry type debris flow, 31T. Note the silt layer around the top of the bulge showing aspect of curve. Gypsum	
wedge. Width of view is 22mm	27
· · · · · · · · · · · · · · · · · · ·	21
Figure - 14. Sample 45. The bottom deposit may be a wet type deposit, and is overlain by a dry type deposit with a basal traction gravel	30
Figure - 15. Detail of contact between the two deposits, 45T. The lower deposit	30
• •	
has been folded slightly at the contact, below the traction gravel. Gypsum wedge. Width of view is 17mm	30
Figure - 16. Detail of folded sand lens in 45T above the locking zone in the	50
traction gravel. Gypsum wedge. Width of view is 22mm	31
Figure - 17. Detail of faulted and brecciated silt layer in 45B. Note the fluid escape	
Figure - 17. Detail of faulted and directiated silt layer in 43D. Note the fluid escape	

channel (light areas). Gypsum wedge. Width of view is 22mm	31
, , , , , , , , , , , , , , , , , , , ,	33
Figure - 19. Detail of 53T showing lattisepic clast fabric. Two directions of dip	
are 30 to 45° to the left and 60 to 90° to the right. Gypsum wedge. Width	
of view is 22mm	33
Figure - 20. Detail of 53B showing skelsepic fabric around a large phyllite clast.	
Gypsum wedge. Width of view is 22mm	34
Figure - 21. Detail of 53B showing a short silt tail around a clast. Width of view is	
8mm	34
Figure - 22. Detail of 53T showing a fluid escape structure from under a small class	st.
Gypsum wedge. Width of view is 22mm	35
Figure - 23. Thin sections of sample 70. Actual size	35
Figure - 24. Detail of top of 70B showing weak omnisepic clast fabric. Gypsum	
wedge. Width of view is 22mm	36
Figure - 25. Detail of 70T showing lattisepic clast fabric. Gypsum wedge. Width	50
of view is 22mm.	36
Figure - 26. Detail of 13B showing laminations and small shale clasts imbricated	30
upslope. The clasts show a weak omnisepic clast fabric. Gypsum wedge.	
Width of view is 22mm	40
Figure - 27. Detail of 13T showing a silt wisp terminating as a halo around a small	
clast. This feature is interpreted to be a fluid injection structure, and is	
discordant with the laminations. Gypsum wedge. Width of view is 22mm.	
(photo	40
Figure - 28. Cartoon of sample 50 showing facies I - V. Crescentic marks are saw	70
marks. Actual size.	41
Figure - 29.Detail of debris flow 2, sample 50. Note the omnisepic clast fabric,	41
·	
décollement surface, and thin laminations. Gypsum wedge. Width of view is 22mm	41
	41
Figure - 30. Detail of base of debris flow 3, section 50B. Silt tails around a small	40
clast and silt wisps. Gypsum wedge. Width of view is 8mm	42
Figure - 31. Thin sections of sample 28 showing a silty facies I at bottom and a	40
cobbly facies II at top. Note large sand clast in 28B	42
Figure - 32. Detail of left side of 28B showing thin laminations, omnisepic	
microclast fabric, and faulting from melting of underlying ice. Width of	4.
view is 17mm.	46
Figure - 33. Detail of 28B, showing sand intraclast and thin laminations with	
omnisepic clast fabric. Width of view is 22mm.	46
Figure - 34. Detail of 28T showing base of facies II. Thin laminations are present	
under the larger clasts. A fluid escape structure is present to the right of	
the micrograph, which disrupted the silt laminations. Gypsum wedge.	
Width of view is 22mm	47

INTRODUCTION

Micromorphological analysis of glacial sediments has been used in previous studies to differentiate genetic types of till. In North Sea glacial deposits, "flow tills" have been differentiated from a basal lodgement till on the basis of microstructures (van der Meer and Laban, 1990). Additionally, micromorphology has been used to characterize tectonic deformation of basal tills associated with a deforming bed (van der Meer, 1993), and to elucidate subglacial conditions and processes acting on tills (Menzies, 1990; Menzies and Maltman, 1992). The use of this technique to determine sedimentary genesis in Pleistocene and recent glacial deposits, however, has not been pursued extensively.

Considering the paucity of information on the micromorphology of glacial sediments, the present investigation was undertaken. The purpose of this study is twofold:

1) to utilize micromorphological analysis to inventory and characterize microstructures found in contemporary subaerial glacigenic debris flow deposits, and 2) to differentiate the microstructures representative of dry-type debris flow deposits from those of wet-type debris flow deposits. Dry-type debris flow deposits, as used in this study, correspond roughly to Lawson type I and II flow deposits, and wet-type debris flow deposits correspond roughly to Lawson type III and IV deposits (Lawson, 1979, 1982; see below for debris flow type characteristics). It is the hypothesis of this study that

micromorphological analysis will allow the differentiation of contemporary dry-type from wet-type debris flow deposits formed at the terminus of the Matanuska Glacier.

SITE DESCRIPTION

The Matanuska Glacier is located in south central Alaska (Figure 1), approximately 140 km north of Anchorage at 61° 47′ N, 147° 45′ W. The glacier flows northward 40 km from the ice fields in the Chugach Mountains and terminates at the East-West trending Matanuska valley. The terminus of the glacier is comprised of a stagnant supraglacial debris-covered ice zone and an active white ice zone. Proglacial sedimentation is occurring near the active ice zone in what is called the western terminus region (Lawson, 1979).

Near the terminus the glacier flows out of an overdeeping, and significant volumes of debris are incorporated into the ice mass as freeze-on occurs at the base of the glacier (Strasser et al. 1996). Freeze-on produces debris rich basal ice, with debris concentrations up to 74% in the stratified basal ice facies (Lawson, 1979). When basal ice ablates during warm weather, water saturated debris is released, undergoes fluidization and liquefaction, and produces debris flows. Debris is generally resedimented several times after release from the ice and comprises the majority of deposits at the terminus (Lawson, 1979, 1982).

LITERATURE REVIEW

Glacigenic debris flows have been investigated and reported in the literature by several researchers, most notably by Hartshorn (1958), Boulton (1968), Marcussen (1973, 1975), Evenson (1977) and at the Matanuska glacier by Lawson (1979, 1982). Many debris flow deposits were originally interpreted as a "till", and hence were given the name "flow till" (Hartshorn, 1958) as their flow origin was illuminated. As the term "till" implies glacially derived sediments deposited *in situ*, the use of "debris flow" is a more accurate term for resedimented debris (Lawson, 1982). However, "flow till" will be presented in this summary when used by the original author cited, and is here used interchangeably with "debris flow".

Hartshorn (1958) was the first to recognize the significance of flow tills produced by Pleistocene ice sheets. In the areas Hartshorn studied in Southeastern Massachusetts, debris flows often overlay fluvial stratified drift, and were originally and incorrectly interpreted by other workers as lodgement till associated with a readvance of the ice sheet. In these locations, the debris flows appeared structureless at the macroscale. Boulton (1968) described flow tills being presently deposited on proglacial outwash sediments at the margins of some Vestspitsbergen glaciers, in a manner that produced sequences similar to those described by Hartshorn in Massachusetts (1958).

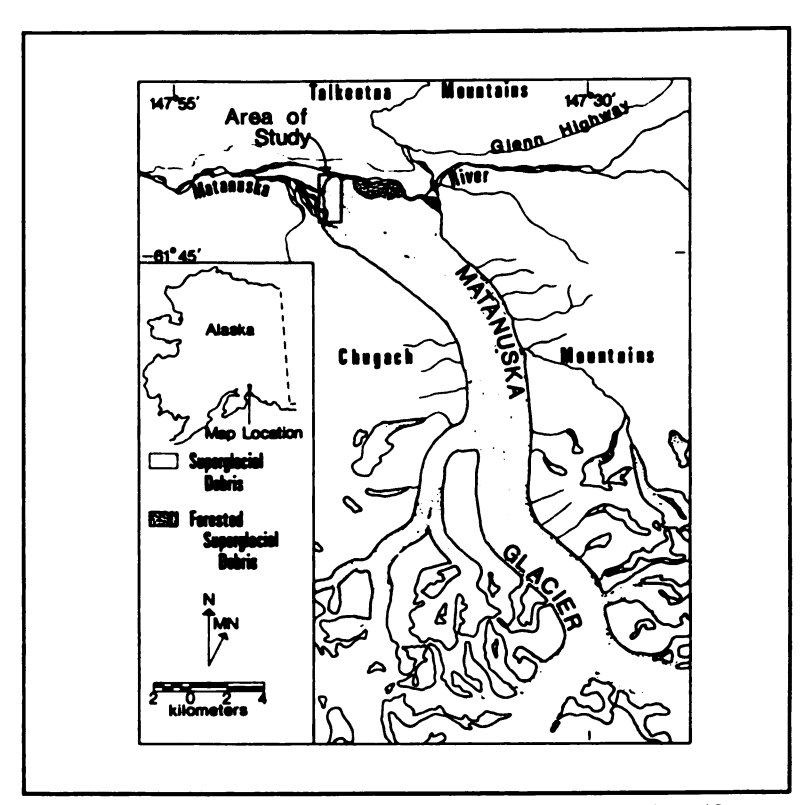


Figure 1. Map of the Matanuska Glacier and Alaska. (from Lawson, 1979)

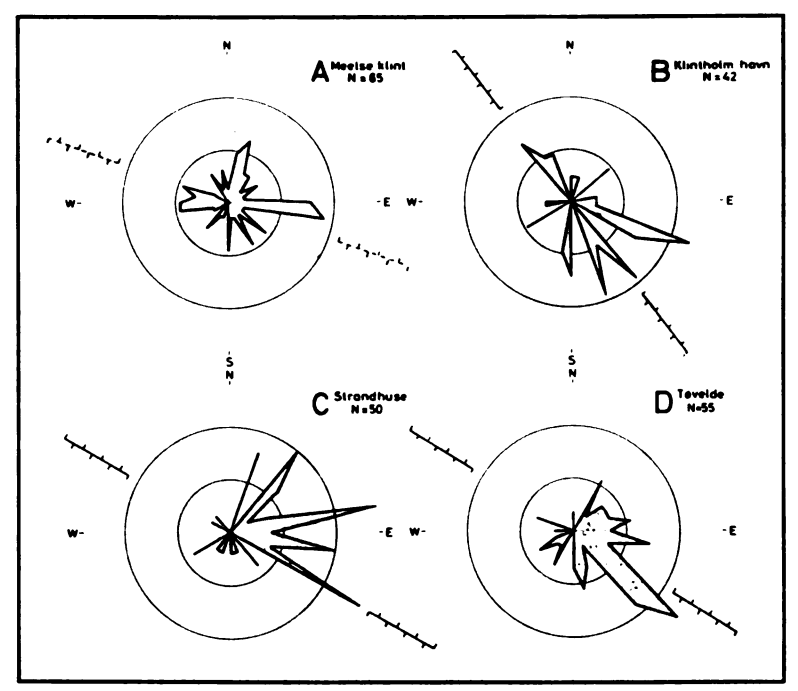


Figure 2. Stereograms of flow till fabrics. (From Marcussen, 1975)

In the Vestspitsbergen glaciers, debris was supplied from englacial debris bands exposed at the termini that originated from compressive flow, and which dip steeply upglacier. The debris bands contain upwards to 80% debris by volume and contain rounded and subrounded clasts, which Boulton interpreted to be derived from the glacier bed. During ablation of the englacial ice and debris bands, debris was released and formed saturated flows which were deposited in low areas on glacier ice or ice-cored moraine, some which flowed off the ice onto proglacial sediments.

Boulton (1968) outlined three modes of movement of subaerial flow tills, which are governed by several variables such as grain size, water content, topographic position, and whether the sediment/till interface is frozen. The first mode occurs when superglacial debris of a low water content rests on melting englacial ice. The contact between the debris and the ice acts as a shear plane in which the sediment moves slowly downslope as a cohesive mass. If water content is higher, the flow moves downslope through differential shear as a lobe, which moves rapidly and exhibits a clast fabric parallel to flow direction in the body of the flow. On saturated sediments on the ice surface, very thin flows form on small angle slopes of 1°-2°. If water content is high enough, surface streams may form which can carry fines from the debris flow.

Most significantly, Boulton (1968) advanced the idea that many till deposits previously interpreted to be subglacial may in fact be of superglacial and proglacial debris flow origin. Consequently, many multi-till sequences seen in Pleistocene glacial deposits originally interpreted to represent multiple advances and retreats may in fact be debris flows associated with a single advance and retreat cycle.

Marcussen (1973) described subaerial flow till deposits occurring over and interfingered within fluvial sands and gravels in Denmark. In the Danish locations, the flow till was often stratified and contained a fabric parallel to subparallel to stratification, which Marcussen attributed to laminar flow in a water-rich environment. Spatially, the flow tills were deposited on what were interpreted to be kame and kame terrace environments, in addition to deposition in outwash basins.

The first geotechnical data of flow tills was presented by Marcussen (1975) in an attempt to distinguish flow till from lodgement till in Denmark. Fabric diagrams (Figure 2) of flow tills show a random and poorly developed orientation which is consistent with the constantly changing topography of the ablating ice-proximal environment. The lack of a consistent fabric results most likely from a sampling of several depositionally distinct small debris flows within a larger deposit. It should be noted however, that individual flows moving under differential shear would have an ordered fabric parallel to flow direction, as shown by Marcussen (1973) and Lawson (1979). Conversely, lodgement till provided more consistent and ordered fabric diagrams on the scale of sampling.

DEBRIS FLOW CLASSIFICATION AT THE MATANUSKA GLACIER

At the terminus of the Matanuska Glacier, the source for most debris flows is the ablation of debris-rich basal ice. Debris flowage is also initiated from the saturation of a sediment pile on the glacier ice or ice cored moraine (Lawson, 1979). Additionally, several occurrences of debris flows initiated from the ablation of debris bands on the glacier surface were observed by the author, similar to flows reported by Boulton (1968). Due to the large amount of available water from melting ice, these flows were generally very thin (<10cm), and may be preserved if they flowed onto proglacial sediments.

Subaerial debris flows forming at the Matanuska Glacier have been classified into four types by Lawson (1979, 1982), primarily as a function of water content (see below). Flow of debris is initiated when the saturation of the sediment reduces the shear strength to failure. Debris flows are transported down slope, often in channels, and deposited when the slope becomes horizontal or saturation ceases. The following characteristics are summarized in **Table 1**.

Type flow characteristics

Type I flows have a water content of 8 - 14% by weight, are non-channelized, and are characterized by cohesive plug flowing over a thin (a few cm) basal shear zone.

Table 1. Characteristics of type debris flows. (After Lawson, 1979)

Sediment	Bulk texture		Internal organization			Contacts and	Pene-	maximum observed dimensions
flow type	Type 1) Mean (4) 2) Std dev (4)	General	Structure	Pebble fabric	Surface forms	basal surface features	contemporaneous deformation	(length×width, thickness, m)
-	Gravel-sand-silt, sandy silt 1) -1 to 2 2) 3 to 4.5	Clasts dispersed in fine-grained matrix.	Massive.	Absent to very weak; vertical clasts. $S_1 \approx 0.49-0.55$	Generally planar; also arcuate ridges, secondary rills and desiccation cracks.	Nonerosional, con- Possible subflow formable contacts; and marginal decontacts sharp; formation during load structures.	Possible subflow and marginal deformation during and after deposition.	Lobe: 50×20, 2.5
=	Gravel-sand-silt, sandy silt, silty sand	Plug zone; clasts dispersed in fine-grained matrix.	Massive; intrafor- mational blocks.	Absent to very weak; vertical clasts.	Arcuate ridges; flow lineations, marginal folds, mud volcanoes,	Nonerosional, conformable contacts; contacts indistinct to sharp; load	Possible subflow and marginal deformation during and after deposi-	Lobe; 30x 20, 1.5; sheet of coalesced deposits.
	2) 3 to 4	Shear zone; gravel zone at base, upper part may show de- creased silt-clay and gravel con- tent; overall, clasts in fine- grained matrix.	Massive; deposit may appear layered where shear and plug zones distinct in texture.	Absent to weak; bimodal or multi- modal; vertical clasts. \$\frac{1}{2} \text{ a} 0.50-0.65	braided and distributary rills on surface,	structures.	tion.	
≡	Gravelly sand to sandy silt 1) -2.5 to 2.5 2) 3.5 to 2	Matrix to clast dominated; lack of fine-grained matrix possible; basal gravels.	Massive; intrafor- mational blocks occasionally.	Moderate, multimodal to bimodal parallel and transverse to flow. \$1 \precedent 0.60-0.70	Irregular to planar; singular rill development; mud volcanoes.	Nonerosional, conformable contacts; contacts indistinct to sharp.	Generally absent; possible subflow deformation on liquefied sedi-ments.	Thin lobe; 20x 10, 0.5; fan wedge; 30x 65, 3.5; rarely, sheet of coalesced deposits.
≥	Sand, silty sand, sandy silt 1) >3.5	Matrix except at base where granules possible.	Massive to graded (distri- bution, coarse- tail).	Absent.	Smooth, planar; mud volcanoes possible.	Contacts conformable; indistinct.	Absent.	Thin sheet; 20x 30, 0.3; Fills surface lows of irregular size and shape.

Characteristics of sediment flow deposits, terminus region, Matanuska Glacier, Alaska.

*Length and width refer to dimensions parallel and transverse to direction of movement prior to deposition.

Thicknesses range up to 2 m, sorting is poor, and clasts are often found supported in a fine-grained matrix. Surfaces of type I flows may have angles up to 45° in the marginal and frontal slopes areas.

Type II flows are characterized by a water content of 14 - 19% by weight, and are generally channelized. As with type I, plug flow occurs over basal and lateral shear zones where laminar flow is dominant and which contain normal-graded tractional gravels.

Thicknesses are up to ~1.5m, sorting is poor, and texture is similar to type I flows.

Surfaces of type II flows can hold angles similar to type I flows. Pore fluid expulsion channels (1-2 mm diameter) occur in clusters in the plug zone. If the water content is higher, flow can be more plastic than in type I flows.

Type III flows have a water content by weight of 18 - 25%, are channelized, and flow by differential shear throughout, although thin discontinuous plugs may be present if water content is low. These flows are thinner (0.5 m. per lobe), and hold surface angles less than those possible for type I and II flows. Grain size fines downflow, particles often are imbricated up slope. As type III flows often occur in meltwater channels, small lenses of fluvial sediments may be intercalated. Clasts in low-viscosity debris flows (such as wetter type II and type III) sink and concentrate in horizons (Marcussen, 1973, citing Boulton, 1971).

A debris flow with greater than 25% water by weight is considered a type IV debris flow. Flow often follows meltwater channels, is laminar throughout, and is often fully liquefied. Thicknesses of individual flows are thinner than other flow types, and hold near horizontal or horizontal slopes. A fine grained flow body overlies similar fine-grained

silt and sandy silt traction particles. After flow has ceased, loss of pore fluids and grain settling would have a tendency to destroy flow structures and fabric, but may allow for the grading of particles.

Figure 3 demonstrates the relationship between mean grain size and water content in debris flows. Mean grain size decreases significantly between water contents of 8 and 17%, roughly corresponding to type I and type II flows (Lawson, 1979, 1982). Generally, the mean grain size in thin section can therefore be used qualitatively to estimate formational water content and debris flow end members.

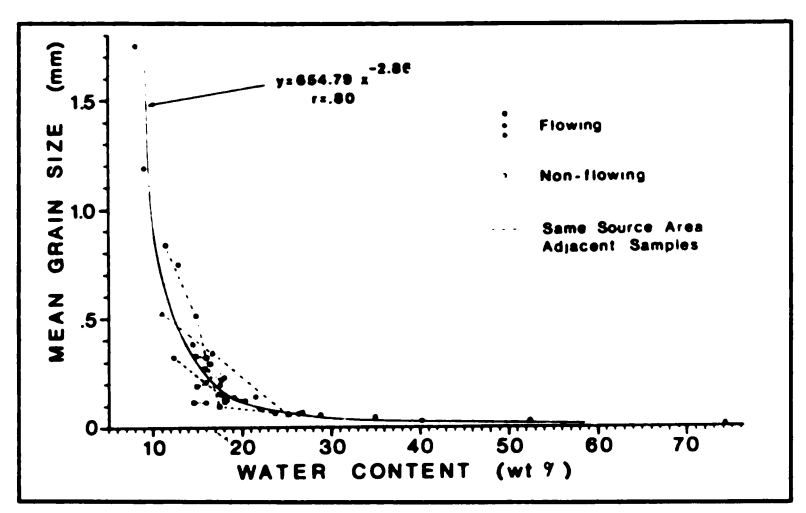


Figure 3. Mean grain size of debris flows as a function of water content. (From Lawson, 1979)

Theoretical microstructures of debris flow deposits

Microstructures in debris flow deposits can be of four varieties: 1) structures formed during debris flow, 2) structures formed during debris deposition, 3) structures inherited from the parent deposit, and 4) postdepositional structures. Differentiating inherited structures from flow or depositional structures may be difficult in some dry-type samples. For example, a type III flow may have been deposited on ice which subsequently

melts and initiates a type I flow. In this situation, if plastic deformation of the plug in the type I flow was minimal, the thin section would show type III structures.

Microstructures expected to be found in type I and II flows include laminar shear structures at the base of the flow, load structures if the debris flow overrode a deformable substrate, pore fluid expulsion channels, brittle to plastic flow structures, intraformational sediment blocks of random orientation dispersed throughout the matrix, lag gravels, and a poorly to well defined clast fabric. Some of these hypothetical structures have been previously postulated by Hampton (1975); the rest belong with the author.

Considering the higher water content in type III flows, microstructures expected to be found would include laminar flow structures (laminations), weakly to strongly defined clast fabric (Hampton, 1975), upslope imbrication of clasts, good sorting, silt wisps and tails, and pore fluid expulsion channels.

In thin section, type IV deposits would be expected to show homogenous texture and a lack of observable flow or deformation structures, although some flow structures may be preserved.

MATERIALS AND METHODS

Sampling protocol

Samples were taken from debris flow deposits with metal Kubiena tins, small rectangular boxes (750mm x 500mm x 400mm) with two open ends, and accompanying lids. After a sample site was chosen for a suitable debris flow deposit, a vertical face was cleared and an open end of a Kubiena tin was placed on the surface. Sediment surrounding the tin was carefully cut away with a knife, and the tin was slowly pushed over the remaining sediment block until filled tightly and completely by sediment. Tins were not forced into the sediment to avoid structural disturbance during sampling. The tin and sediment were then removed from the deposit, and excess sediment was trimmed away until covers could be put on the two open sides of the tin. Location, sample number, and orientation of the sample were marked on the tins and in a field notebook. Tins were numbered and placed in airtight plastic bags to prevent desiccation. Transportation of the samples from Alaska may have resulted in some disturbance, which should not have greatly affected the micromorphological orientation of particles.

During sampling, an attempt was made to sample contacts between depositionally distinct units. Cobble-rich deposits could not be sampled using Kubiena tins, and therefore are under-represented in this study. However, these deposits did not appear to differ from

cobble-poor deposits in macro-texture, structure, or composition, and are therefore not considered to be genetically distinct from the types of debris flow deposits sampled.

Sample and thin section preparation

Samples were impregnated under vacuum with a polyester resin using Cobalt

Napthenate as an accelerator and Lupersol DDM-9 for a catalyst. The interested reader is
referred to Bouma (1969) for further details of the impregnation process. Hardened
sediment blocks were thin sectioned and photomicrographs prepared using a Petroscope
with multiple magnifications and a 35mm camera. A bottom and a top thin section were
made from each sample, and are designated in the text with a B or a T following the
sample number.

Terminology

This study utilizes terminology developed by Brewer (1976) and interpretations of van der Meer (1987, 1990, 1993) and the author to describe thin sections. Microstructure types can be grouped into fabric, laminar, plastic, brittle, and miscellaneous structures. Structures found in this study are illustrated in **Figure 4** (Menzies, Lachniet, unpublished, adapted from van der Meer, 1993).

The fabric terminology was originally developed by Brewer (1976) to describe plasma (clay-sized sediment) fabrics. In the Matanuska debris flow deposits, plasma sized material is generally not present, so the plasmic terminology has been extended to include clastic fabrics. In this study, clast size ranges from large silts to clasts the size of the thin

section. In Brewers' soil terminology, 'skeleton' grains are clasts generally larger than fine silt and are distinguished from the finer grained plasma or matrix. Skelsepic clast fabrics consist of orientations of smaller grains and clasts parallel to the surface of a larger 'skeleton' clast. Skelsepic clast fabrics are developed during rotational movement of the 'skeleton' or 'core' clast under laminar or plastic conditions. Lattisepic clast fabric consists of the apparent long axes of clasts dipping in two directions forming a lattice-like arrangement. Lattisepic clast fabrics are developed under plastic to semi-plastic conditions. Omnisepic clast fabrics consist of most or all of the clasts exhibiting a uni-directional aspect and are interpreted to form under laminar conditions (this study).

Generally, skelsepic, lattisepic, and omnisepic clast fabrics form under a continuum of stress from high to low respectively, which can be roughly correlated to dry to wet conditions in this study.

Laminar microstructures are formed during flow under wet conditions and are expressed as thin (<3 mm) laminations within a deposit. Décollement surfaces form at the basal layer of a flow under wet conditions as the body is separated from and flows over a traction gravel or underlying deposit. Silt wisps form as a silt clast or inclusion becomes elongated into a thin lineation during laminar or plastic flow. Silt tails are a variety of silt wisps that occur in association with a rotating silt-coated clast.

Plastic (or ductile) structures form under pressure in sediments with intermediate water contents. Examples are fold structures, rotational structures ("milky way structures"), strain caps and shadows, and necking structures. Fold structures are formed under compression of cohesive sediments. Strain caps and shadows are believed to be

formed from rotation due to shearing (van der Meer, 1993). Necking structures are essentially a variation of a skelsepic clast fabric, but may also be formed during fluid expulsion in channels between clasts (van der Meer, 1993).

Brittle structures form as a result of stresses on a dry or cohesionless sediment.

Faulting, shearing, and brecciation are the most common manifestations of brittle structures in the Matanuska debris flow deposits, and are most commonly post-depositional.

Miscellaneous structures are represented by fluid escape channels, which are common in debris flow deposits of the Matanuska Glacier. Fluid escape channels are generally vertical to subvertical, but can be horizontal if water movement is redirected by a relatively impermeable bed. In these channels, fines are removed by 'washing' and the resulting channel sediment is fine to coarse sand. The silt-rich water can be injected into fractures, planes of weakness, or pores within the sediment, and results in a concentration of fines. Structures formed in this manner are here called "fluid injection structures".

Many pebble to cobble sized clasts show a halo, or a ring of silt around their edges. These haloes may form as a coating of wet silt on the clast, or as a result of rotation of the clast within the matrix (van der Meer, 1993). Observations in this study indicate that higher water content flows generally have thinner or non-existent haloes, as the cohesion of the debris/water slurry decreases with increasing water content.

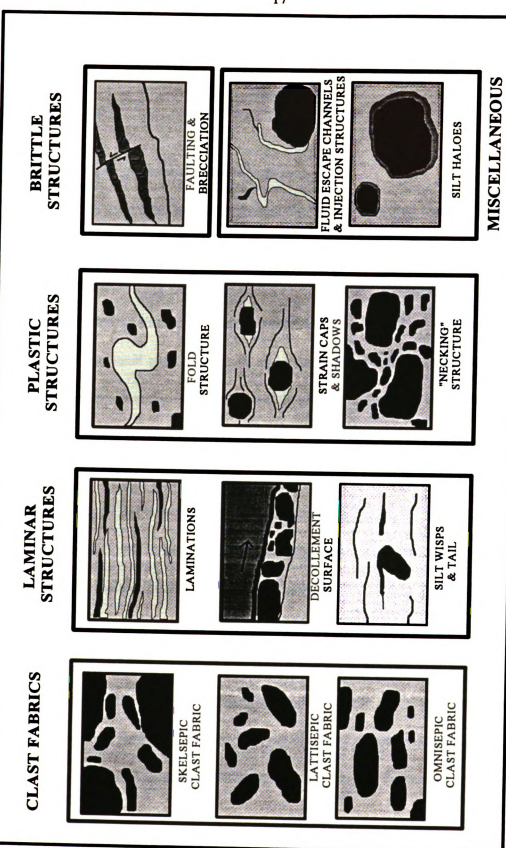


Figure 4. Debris flow deposit microstructures. Adapted from van der Meer (1993) by Lachniet and Menzies

RESULTS

Moraine site description and sample locations

Figure 5 shows the western terminus region and ice-cored moraine of the Matanuska Glacier, as determined from aerial photographs. Sample locations and major morphological features are noted. The majority of samples were taken from the unvegetated ice-cored moraine, which is comprised of several tall (5 - 10 m) eroding ridges, low areas, small stream channels, and seasonally or historically inundated lake areas. The moraine is composed predominantly of older deposits in the ridges, deposited when the ice margin abutted the moraine, and of recent resedimented debris flow deposits in low areas. Debris flow deposits in the ridges are highly variable in character and range from type I to type IV. Wet-type debris flow deposits are often found next to and intercalated with fluvial lenses (sometimes crossbedded) and meltwater silts produced by sheet flow. The meltwater silts are generally finely laminated (<1mm -2mm) and often contain injection structures. Where the silts were overridden by dry-type debris flows (generally type I and II (Lawson, 1979), they are often highly folded and faulted. The occurrence of type III and type IV flows in association with fluvial and meltwater deposits indicates they were formed under very wet conditions at or near the ablating ice terminus.

On the moraine area, deposits are commonly reworked frequently, often several

times within a season (Lawson, 1979, 1982). For this reason, debris flow deposits still retaining a lobate surface shape on the moraine are probably recent in origin. These recent resedimented debris flow deposits are more homogeneous in character, and represent flows with low water content (types I and II). In a general sense, the most common type of debris flow now forming on the moraine represents a reworking of older morainal sediments from the higher ridges, and lower areas near a source of water. In these deposits, the morphology is lobate and not channelized, often with compressive ridges at the toe. The upper surface of the debris flow deposits can have slopes up to 40°, and often contain vesicles, which may be formed from the expulsion of liquids or gases during flow and deposition. Generally, clasts are present but the debris flow deposits are matrix supported. The deposits are mainly comprised of a silt matrix and assorted pebble to cobble sized clasts that may or may not exhibit a clast macrofabric. The predominance of type I and II recent debris flows may be attributed to the much drier conditions away from the ablating ice terminus. Small kettle lakes (<5 m diameter) occur in some high areas of the moraine, and may provide the water to undermine the morainal ridges and initiate debris flow formation.

In the lowest areas near to stream baseline (either current or previous), some morainal areas were inundated with water during periods of high glacial discharge or ponding. Consequently, lacustrine sands, silts, and clays were deposited, often in association with debris flows. Lacustrine sediments are found in two main locations on the moraine, the Lake area and the Old Lake area. A summary of samples collected is shown in Table 2

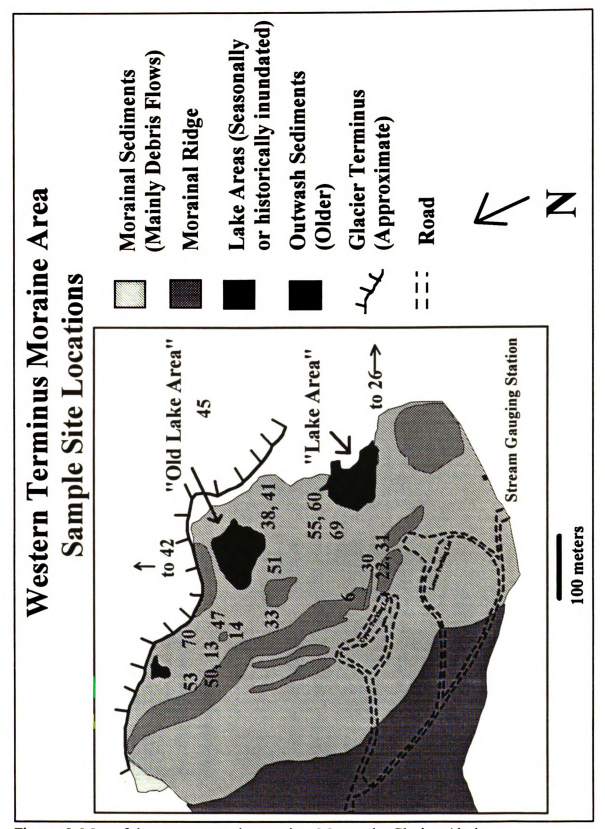


Figure. 5. Map of the western terminus region. Matanuska Glacier, Alaska.

Table 2. Sarr	Fable 2. Sample information						
Sample no.	9	13	14	22	28	30	31
# of units]	I	2	2	2	2	2
				;	dry-type debris flow deposit		debris flow
	dry-type debris flow	wet-type debris flow	dry-type debris flow	mettwater sifts, debris	debris flow	debris flow deposit, deposit, meltwater	deposit, meltwater
unit description	deposit, meltwater silts	deposit	deposit, unknown flow deposit		deposit (28B)	meltwater silts	silts
Thần sections	попе	13B&T	14B&T	PROU	28B&T	1.480E	31B&T

Sample no.	33	38	41	42	45	47	20
# of waits	7		I	1	2	1	3
		subaquatic debris	subaquatic debris	meltwater silts, highly	dry-type debris flow deposit mettweter silts, highly (45T), wet-type debris flow		3 wet-type debris
unit description	2 debris flow deposits	flow deposit	flow deposit	folded	deposit (45B)	debris flow deposit flow deposits	flow deposits
Thin sections	none	none	none	42B&T	45B&T	none	50B&T

Sample	15	83	SS	09	69	20	total# of un
# of units	1	1	l	3	2	1	
unit description	fluvial sands and gravels	dry-type debris flow deposit	dry-type debris flow subsquetto debris deposit	subaquatic debris flow deposit	dry-typi subequatic debris flow deposit deposit	dry-type debris flow deposit	
Thin sections	SIB&T	S3B&T	DODE	none	69L&R	70B&T	

Deposit type Iry type wet type ubsquatic	Sample no. 6, 45T, 28T, 31, 53, 70, 14 13, 28B, 50, 45 38, 55, 60, 69, 41
dher	6, 14, 22, 30, 31, 33, 42, 51

Dry-type flow deposit samples

Dry-type debris flow deposits were identifiable in the field by several characteristics. Primarily, a high angle of surface slope and lobate shape are diagnostic, in addition to textural heterogeneity a poorly-defined macro clast fabric. Most of the dry-type debris flow deposits sampled on the moraine were identified according to the characteristics described by Lawson (1979, 1982)

Sample 14 was taken from a recent debris flow deposit originating about 1 m from older slumped deposits near the main morainal ridge. The surface of the deposit is lobate, dips about 10°, and holds a steep angle at the nose. Surface relief is on the order of 0.5cm. The top portion of the flow contains vesicles, which probably originated from fluid expulsion during flow and deposition. The sample contains rounded pebble to cobble sized clasts (<4cm along c-axis) some of which were removed from the sides or back to permit sampling. The lobate morphology and sediment source are consistent with a type I debris flow (Lawson, 1979).

Thin sections made from this sample show two units (Figure 6). The silty lower deposit dips to the right, is bounded by folded sandy layers at the top and bottom, and its genesis is unknown. The top sand layer shows a microclast fabric parallel to the trend of the layer, and is probably fluvial in origin.

The top debris flow deposit is homogeneously sorted silt and sand, and shows stratification dipping about 10° to the left which terminate at the contact with the lower deposit. Small phyllite clasts in the top flow are vertical to subvertical, and a small silt intraclast with vertical silt layers is present.

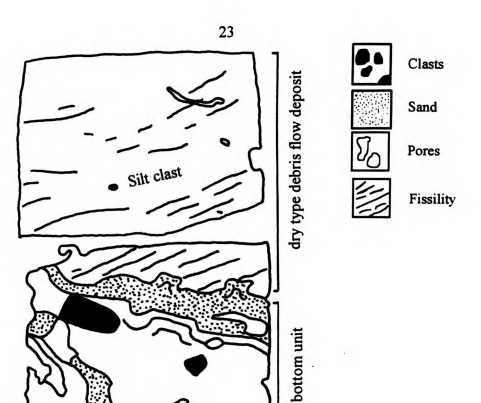


Figure 6. Cartoon of sample 14 showing two units, a deformed bottom unit, and a top dry type debris flow unit. Actual size.

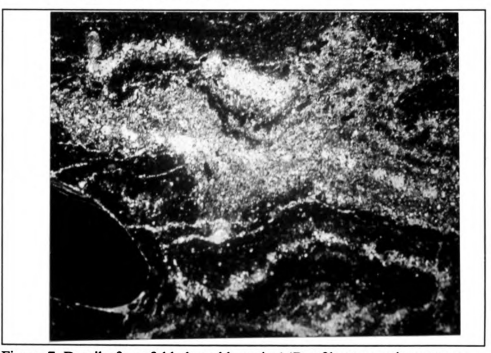


Figure 7. Detail of top folded sand layer in 14B, of bottom unit, gypsum wedge. Width of view is 27mm.



Figure 8. Detail of 14T, dry type debris flow. Note the fissility planes dipping to the left and the silt clast near the center of photo. Gypsum wedge. Width of view is 22mm. (photo 3.25)

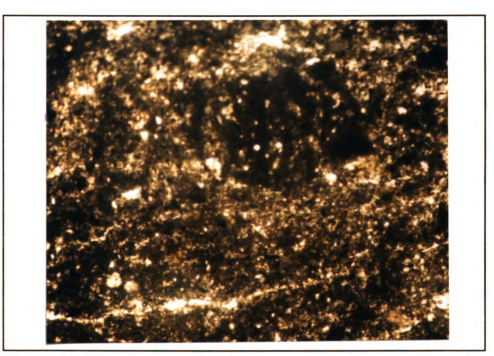


Figure 9. Detail of silt clast in 14T. Note the vertical silt layers. Width of view is 8mm. (photo 3. 26)

Interpretation: The lower sediments were *deformed* (Figure 7) and folded as the top debris flow plastically overrode them. Evidence for plastic or semi-plastic flow in the top deposit is shown by the lack of an omnisepic microclast fabric and fissility planes parallel with flow direction. The fissility evident in the thin sections may have been enhanced from sample processing, but are believed to have followed original planes of weakness (Figure 8). The silt intraclast is present due to *incomplete mixing* of the flow (Figure 9), a characteristic of a low water content flow (Lawson, 1979).

Sample 31 (Figure 10) was taken of a contact between a clast rich debris flow deposit and underlying meltwater silts from a ridge in the south moraine area. The upper debris flow deposit is composed of rounded to subrounded pebble and cobble sized clasts in a silty matrix. Sorting is poor and texture is heterogeneous, flow direction was unknown. The flow appears to have truncated the underlying faulted and deformed silts to form an erosional unconformity. Fine laminations at the base of the debris flow deposit were visible in the field. Considering the characteristics described above, the deposit was interpreted to be a dry-type deposit.

Thin sections made from this sample show several features that are characteristic of a dry-type debris flow deposit. Above the contact with the meltwater silts in 31B, there is a wavy layer of fine silt surrounding a few pebbles, interpreted to be the basal zone of the debris flow deposit. Strain caps and shadows and necking structures surround the pebbles (Figures 11 and 12). A large sediment clast (2 cm) is present in the center right of the thin sections.

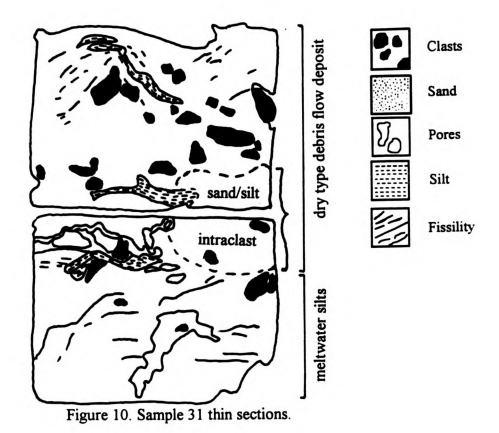


Figure 11. Detail of the contact between meltwater silts and the dry type debris flow in 31B. The silt layers represent the basal zone of shear. Gypsum wedge. Width of view is 22mm.

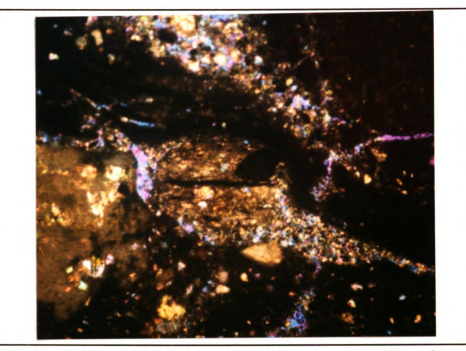


Figure 12. Detail of the basal shear zone from previous figure. Note the strain cap and shadow on the small metamorphic clast. Gypsum Wedge. Width of view is 8mm.



Figure 13. Detail of deformation bulge in the dry type debris flow, 31T. Note the silt layer around the top of the bulge showing aspect of curve. Gypsum wedge. Width of view is 22mm.

The body of the debris flow deposit contains many clasts with *no consistent long* axis fabric. Fissility (possibly process enhanced) and a discontinuous silty layer show a bulge around a pebble clast (Figure 13).

Interpretation: The upper debris flow deposit is a dry-type flow that overrode meltwater silts. The silty layers and plastic flow structures at the base of the flow represent the basal shear zone of the deposit. The wavy morphology of the basal silt layers formed as the flow overrode the irregular surface of the meltwater silts. The bulge in the top left of 31T formed during *compressive flow* as the body of the deposit encountered a locking zone, possibly caused by the slower moving *sediment intraclast* to the right of the thin sections. The sediment intraclast is present due to *incomplete mixing* of the flow. In this scenario, two dimensional movement was from left to right.

Sample 45 was taken on the debris-covered ice area from a silty debris flow deposit with some subhorizontal stratification and a sandy layer. The sediment is underlain by basal ice. In the field, only one depositional unit was recognized, but two distinct units are observable in thin section (Figure 14).

The bottom unit is a homogeneous fine silty sand, which contains discontinuous and irregular silt layers and silt wisps. The main silt layer appears brecciated and the right side is faulted upward 0.5 cm. Linear sandy layers and pores are visible throughout the bottom unit. No microfabric was obvious in thin section. The upper surface of the bottom deposit is irregular and slightly folded (Figure 15). In 45T, a sand and gravel layer with intermixed silt and no apparent clast fabric dips about 5° to left. Above this is silty sediment with sub-horizontal silt wisps and one obvious folded sand layer.

There are several small clasts (<10mm) towards the left of the slide that do not appear to have a preferred orientation. The largest clast has a discontinuous halo of fine grained sediment, while the other smaller clasts have weak or no haloes.

Interpretation: The top unit is a dry-type debris flow (I or II) with a tractional gravel at its base. During flow deposition, the gravels surrounding the large clast became locked due to friction and the low water content of the flow. This locking zone caused the sand layer above to be folded, an indication of compressive flow (Figure 16). A lack of a defined clast fabric is further indication of a lack of laminar flow in the deposit.

The bottom unit may be a *type IV* flow deposit, which is characterized by silty sand and a lack of macroscale structure. The pores in this unit follow sandier layers which were most likely formed as *fluid escape channels*, one of which crosses the silt layer, and may have been responsible for faulting it upward (Figure 17). The discontinuous silt layer may be a relic flow structure that was not completely destroyed upon dewatering during deposition, which seems likely as the fluid was expelled via the fluid escape channels and would have avoided the more impermeable silt layer. The irregular upper surface is an indication that it was put under stress as the overlying flow over rode it. It should be noted, however, that the identification of this deposit as a possible type IV is based solely on micromorphology and not field identification.

Sample 53 was taken on the north Moraine area near debris covered ice, from a ridge of silty sediments (slide 5.14-5.15). The unit was sampled normal to the strike of the ridge; flow direction was not known. The sediment appeared structureless in the field. The deposit is poorly sorted and texturally heterogeneous, and composed of silty sand with

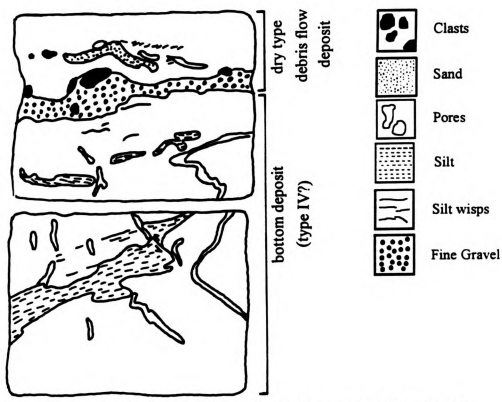


Figure 14. Sample 45. The bottom deposit may be a wet type deposit, and is overlain by a dry type deposit with a basal traction gravel.



Figure 15. Detail of contact between the two deposits, 45T. The lower deposit has been folded slightly at the contact, below the traction gravel. Gypsum wedge. Width of view is 17mm.



Figure 16. Detail of folded sand lens in 45T above the locking zone in the traction gravel. Gypsum wedge. Width of view is 22mm.



Figure 17. Detail of faulted and brecciated silt layer in 45B. Note the fluid escape channel (light areas). Gypsum wedge. Width of view is 22mm.

cobbles ranging up to 20 cm. At the sample face only small pebbles were visible.

Thin sections (Figure 18) of the sample elucidate many structures not visible in outcrop. Angular metamorphic clasts smaller than 1 cm are interspersed throughout the sandy silt matrix along with oblong rounded phyllite clasts less than 0.5 cm long. A rounded phyllite clast (long axis is 4 cm) is present in 53B. The clasts show a *lattisepic* fabric (Figure 19), with the two main axes dipping from 30° to 45° to the left and 60° to 90° to the right. The larger clasts have weakly defined haloes, while around the largest phyllite clast there is a more strongly defined skelsepic fabric (Figure 20).

Interpretation: The reorientation of clasts around the large phyllite clast is evidence that at least some internal deformation of the sediment was occurring, as would be expected for the semi-plastic flow of a dry-type debris flow. Some of the clasts appear to have *silt tails*, as shown in the detail (Figure 21), which are formed from rotation of the clasts. Channels of coarser grained sand are present around some of the clasts, and probably formed as *fluid expulsion channels* during deposition (Figure 22).

Sample 70 was taken on the north moraine area from a debris flow deposit that originated from slumping of older morainal deposits. A trench was dug parallel to flow and the unit sampled parallel to flow. No stratification was visible in outcrop, but a macrofabric was present in which the long axes of the clasts dipped downward away from the source area at an angle approximately parallel to the surface dip of the debris flow. The deposit was matrix-supported but contained many pebble to cobble sized clasts, and some sandy areas in the matrix were also present.

The appearance of the flow deposit is non-channelized, and has a ropy surface

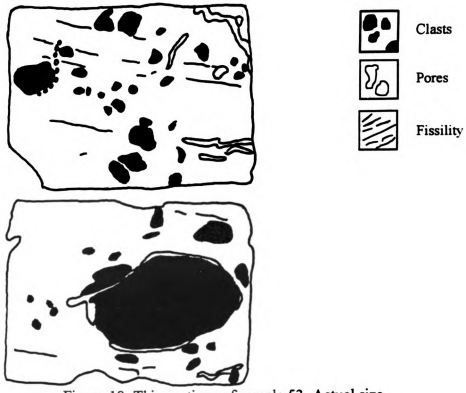


Figure 18. Thin sections of sample 53. Actual size.

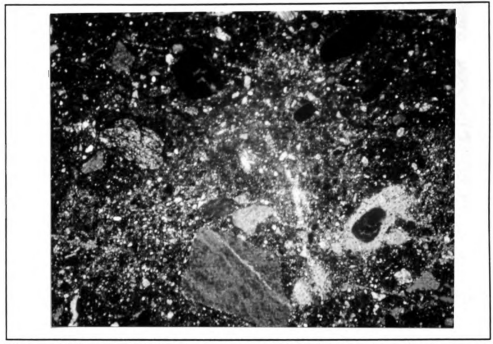


Figure 19. Detail of 53T showing lattisepic clast fabric. Two directions of dip are 30 to 45° to the left and 60 to 90° to the right. Gypsum wedge. Width of view is 22mm.



Figure 20. Detail of 53B showing skelsepic fabric around a large phyllite clast. Gypsum wedge. Width of view is 22mm.

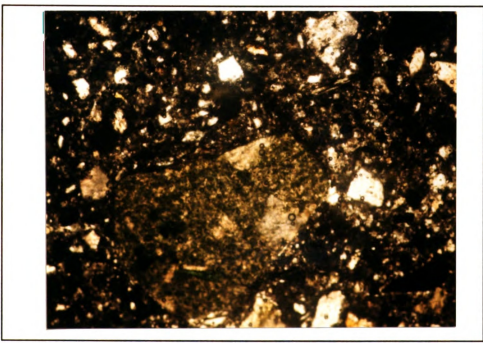


Figure 21. Detail of 53B showing a short silt tail around a clast. Width of view is 8mm.

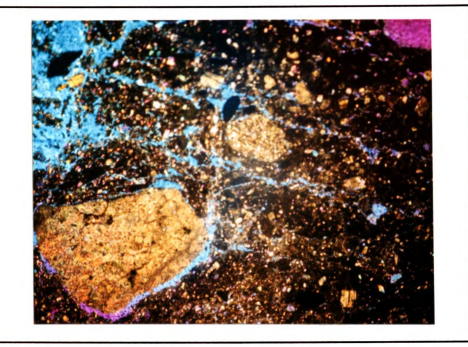


Figure 22. Detail of 53T showing a fluid escape structure from under a small clast. Gypsum wedge. Width of view is 22mm.

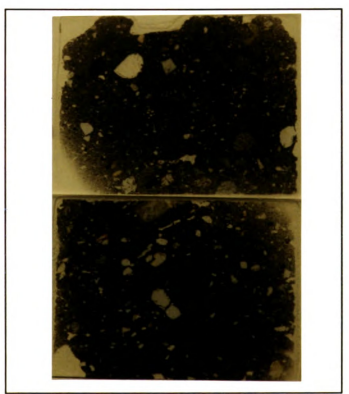


Figure 23. Thin sections of sample 70. Actual size.

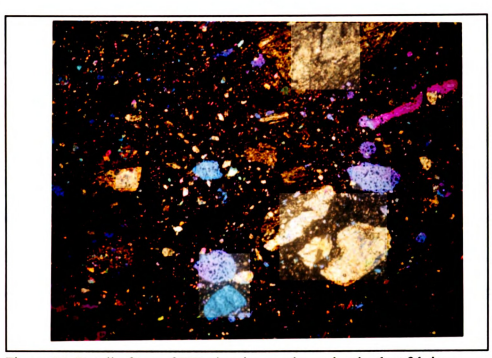


Figure 24. Detail of top of 70B showing weak omnisepic clast fabric. Gypsum wedge. Width of view is 22mm.



Figure 25. Detail of 70T showing lattisepic clast fabric. Gypsum wedge. Width of view is 22mm.

formed from compressive flow. There are several overlapping sublobes of the flow apparent on the surface, and their surfaces dip about 30° away from the sediment ridge.

The flow morphology and sediment source indicate this is a type I flow (Lawson, 1979).

From analysis of the thin sections (Figure 23), it is apparent that there is a well defined micro clast fabric dipping about 30° to the left, with a weaker component with long axes dipping 50° to the right. The clast fabric is generally *omnisepic* (Figure 24) near the base and *weakly lattisepic* (Figure 25) higher in the flow. The transition from an omnisepic fabric near the zone of laminar flow to a lattisepic fabric higher in the flow is an indication of differential shear stresses in the flow deposit. Laminations are not distinguishable. The debris flow deposit is heterogeneous and poorly sorted, and the pores are elongated along dip planes.

Interpretation: This debris flow was initiated when older morainal sediments were wetted enough to reduce cohesion and initiate flow. Considering the high angle of slope upon which this deposit flowed, internal shear stresses were great enough to overcome the plasticity of the plug and semi-laminar flow occurred near the bottom, while semi-plastic flow occurred towards the top. Semi-laminar flow is evident in the well defined clast fabric, which was predominantly omnisepic and semi-plastic flow is shown by the lattisepic fabric component.

Wet-type flow deposit samples

Wet-type debris flow deposits were identified in the field from characteristics outlined by Lawson (1979, 1982). Primarily, a homogeneous, well-sorted texture, and a

well-defined clast fabric were diagnostic, in addition to the presence in some samples of thin laminations. Most of the wet-type debris flow deposits sampled from the moraine area were deposited under wetter conditions at or near the ablating ice terminus.

Sample 13 was taken in the N moraine area from older debris flow deposits in the main morainal ridge. Flow direction was not apparent in the field. The remnant block of debris has crept down about 1.5 m from the original location, and the sample taken is not likely in its original depositional orientation. The debris flow deposit appears massive, well sorted, homogeneously textured, and unstratified on the main face, but on a face normal to this there were some wind sculpted thin laminations (1 - 3 mm) present.

The deposit is matrix supported silt and contains rounded to subrounded clasts with up to a 4cm long axis. Sand and gravel layers are present throughout the sediment block. No macro fabric was apparent in the field. The sorting and texture, along with the thin laminations indicate this is a wet-type debris flow deposit, possibly a type III.

Thin sections 13B and 13T represent one depositional facies, which is thinly laminated and contains sand to pebble sized clasts (<1 cm). Laminations dip to the right, the clasts exhibit a strong *omnisepic clast fabric* and are *imbricated upslope* (Figure 26). Imbricated clasts were reported by Lawson (1979) to be present in type III fan type flows, and seems to be consistent with the observations in this deposit. Figure 27 shows a discordant silt wisp that terminates as a thin halo around a small clast. This feature is interpreted to be a *fluid injection structure* where silt-rich water filled the pore spaces. Clast haloes are generally weakly defined or nonexistent, further indication of a high original water content of the flow.

Interpretation: Sample 13 was transported under laminar flow throughout, as shown by the high degree of sorting, and deposited under wet conditions, possibly in a fan-type setting. The topographic height in the morainal ridge and wet-type structures indicate the deposit was formed when the ice margin abutted the ridge. The thin sections most likely show characteristics of the body of the flow.

Sample 50 was taken from same unit and stratigraphic position as sample 13, from a sediment block located *in situ*, also a wet-type (type III) debris flow deposit. The unit appears massive with a clast fabric dipping slightly downwards and inwards from the outcrop face, which is oriented N-S. From this, flow was estimated to be approximately normal to face. There are five microfacies within this sample (Figure 28), starting from a debris flow in the bottom left corner (I), overlain by a sandy layer (II) which contains some pebbles, a thinly laminated silt (III), another sandy layer (IV), and a thicker deposit (V) filling in the top half of the sample tin. During sampling, the upper right corner was fractured, lost and infilled with loose sediment.

Facies I is wavily stratified with alternations of siltier and sandier layers, is clast poor, and moderately well sorted. Clast fabric is crudely subparallel to the undulating and sometimes discontinuous laminations

Facies II dips slightly to the right, and is composed of pebbles (< 1 cm) in a matrix of silt and sand. Pebble fabric is parallel to the trend of the layer. Fine accumulations of silt wisps cover the pebbles at the top, above which is a finely laminated silt facies (III) with small sand sized phyllite clasts. Clasts have a fabric parallel to the lamination.

Another gravel layer (facies IV) overlies the lower unit which also dips to the right



Figure 26. Detail of 13B showing laminations and small shale clasts imbricated upslope. The clasts show a weak omnisepic clast fabric. Gypsum wedge. Width of view is 22mm.



Figure 27. Detail of 13T showing a silt wisp terminating as a halo around a small clast. This feature is interpreted to be a fluid injection structure, and is discordant with the laminations. Gypsum wedge. Width of view is 22mm.

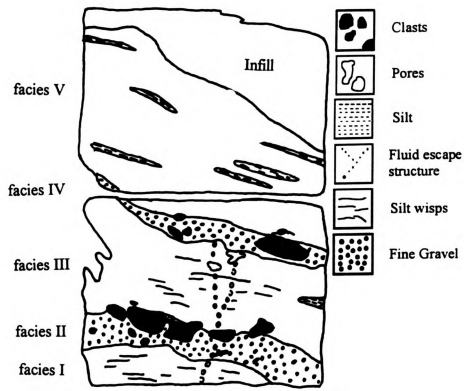


Figure 28. Cartoon of sample 50 showing facies I - V. Crescentic marks are saw marks. Actual size.



Figure 29. Detail of debris flow 2, sample 50. Note the omnisepic clast fabric, décollement surface, and thin laminations. Gypsum wedge. Width of view is 22mm.

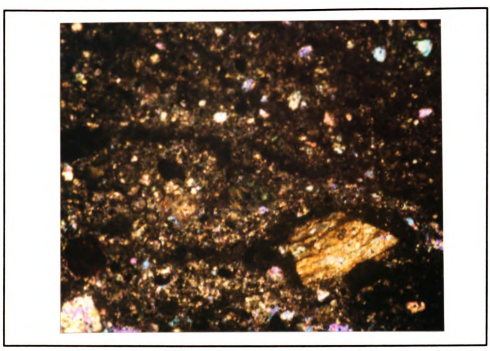


Figure 30. Detail of base of debris flow 3, section 50B. Silt tails around a small clast and silt wisps. Gypsum wedge. Width of view is 8mm.

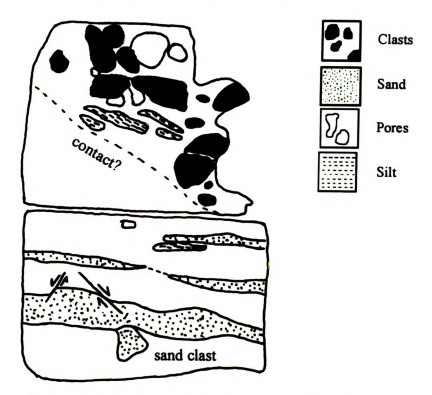


Figure 31. Thin sections of sample 28 showing a silty facies I at bottom and a cobbly facies II at top. Note large sand clast in 28B.

and exhibits a pebble fabric parallel to the trend of the layer. Facies V is finely laminated silt and sand with fine sand sized oblong phyllite clasts dipping parallel to laminations.

Interpretation: Facies I is a wet end member debris flow deposit (debris flow 1) which flowed with shear throughout, yielding the observed micro-clast fabric and thin discontinuous laminations. Facies II is a tractional gravel associated with the debris flow body (facies III) and collectively compose debris flow 2. The silt accumulations and wisps above the gravels represent a plane of décollement where the body of the flow sheared over the tractional gravels, without deformation of the laminations or the gravels. The strongly defined omnisepic fabric and thin laminations are indicative of a wet end member debris flow. A fluid expulsion channel runs vertically through facies I through III and terminates at facies IV (Figure 29).

Above facies III is another tractional gravel (facies IV) with a few silt wisps, associated with the debris flow body of facies V (debris flow 3). Silt wisps are present in the body of debris flow 3 (Figure 30). Again, facies V is thinly laminated with a strongly developed omnisepic clast fabric, indicative of a wet-type debris flow. The top third of 50T shows sediment packed into the tin to prevent sample disturbance. Note that the infilled sediment is disorganized and structureless, except for a few desiccation fractures that do not continue into the debris flow sediment.

Three depositional events are responsible for the facies described in this sample.

Debris flow 1 was deposited and later buried by debris flow 2. After or during the deposition of debris flow 2, a fluid expulsion channel was developed across both debris flows. Debris flow 3 was then deposited above debris flow 2.

Sample 28 was taken at the terminus of the glacier near "site 1". Considering its proximity to the active ice (2m) this deposit is probably very young. The sedimentary sequence consists of a 1 m thick facies I resting on basal ice, and a 10 cm thick facies II at the top. The sample was taken at the contact between facies, and some cobbles were removed to facilitate sampling. Flow direction is not known.

Figure 31 shows thin sections made from this sample. Facies I is a sandy silt, with thin undulating laminations, and small pebble sized clasts exhibiting a *omnisepic fabric* parallel to bedding (Figure 32). The laminations consist of alternating sandy and silty layers, which are slightly faulted to the left of the thin section. The pebbles are dispersed preferentially along laminations, which vary from horizontal to about 15 degrees. Some large cobbles occur in this deposit (c-axis ~15cm). A sand "clast" (1 cm) is present in facies I near the bottom center of 28B, an indication of incomplete mixing of the debris during flow (Figure 33).

Facies II contains many rounded pebbles, and has a visible porosity. In the field, the surface of facies II had a veneer 3mm thick of unknown origin; in some areas there is lag gravel on top, which possibly indicates that this veneer is a product of fluvial sorting/deposition. The thin sections of facies II are poor and not utilizable for micromorphological analysis.

Interpretation: Facies I is a wet end member debris flow as shown by the laminations and clast fabric. The internal organization of the facies I deposit reflects the highly laminar nature under which it flowed, possibly as a continuum of meltwater and debris flow sediment deposition, an observation consistent with a type III flow (Lawson,

1979). The sand clast is a relic of the original sediment source which was not disaggregated during flow. Melting of basal ice caused slight faulting of the sample. The contact between the two facies is indistinct, but may be just below the coarser pebbles at the top of 28T, and dipping 35° to the right. Silt wisps and laminations just below these gravels may represent a décollement surface (Figure 34).



Figure 32. Detail of left side of 28B showing thin laminations, omnisepic microclast fabric, and faulting from melting of underlying ice. Width of view is 17mm.



Figure 33. Detail of 28B, showing sand intraclast and thin laminations with omnisepic clast fabric. Width of view is 22mm.

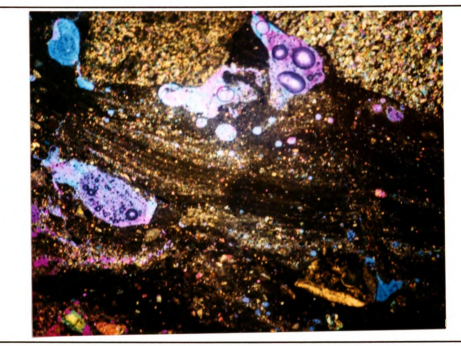


Figure 34. Detail of 28T showing base of facies II. Thin laminations are present under the larger clasts. A fluid escape structure is present to the right of the micrograph, which disrupted the silt laminations. Gypsum wedge. Width of view is 22mm.

DISCUSSION

Debris flow deposits of low water content (Type I and II) have characteristic microstructures that allow differentiation from high water content flow deposits (type III and IV), which are listed in **Table 3**. Of primary interest in distinguishing dry-type from wet-type debris flow deposits in a sediment sequence is the contact between the debris flow deposit and underlying sediments, in addition to the nature of the lag gravel-plug interface.

Characteristics of dry-type debris flow deposits

Type I and II flows demonstrate plastic deformation of the plug when a "locking zone" is encountered in the lag gravel or on surface irregularities of the underlying sediment. Evidence of this deformation is shown by the folding of layers and skelsepic fabric around larger clasts, which other workers have attributed to clast rotation (van der Meer, 1993). Compressive flow structures are observable both in the field on the macro scale, and in thin section on the micro scale.

Microdeformation of underlying sediment is apparent in thin section as faulting, folding, mixing, and fluid escape structures. During flow, sediment from other sources can

be incorporated into the debris mass (Lawson, 1979, 1982) and is completely or incompletely mixed. Microscale sediment clasts of this type are often present in thin section.

A poorly defined clast fabric is observed in some samples and results from internal deformation of the plug during flow. Plasticity of the debris flow generally does not allow the formation of omnisepic fabric (with the exception of flows on high angle slopes, see sample 70), but lattisepic fabric is quite common.

Semi-plastic flow of parts of the plug and a weak clast fabric may develop in type I and II flows if the slope of the debris surface is sufficiently steep. The presence of microstructures in dry-type flow, it should be noted, may be inherited from the sediment source and not produced as result of flow or deposition. The higher cohesion of sediment in a dry-type flow allows the formation of thicker haloes around clasts.

Characteristics of wet-type debris flow deposits

Wetter debris flow deposits show characteristics that contrast with those of dryer debris flow deposits. Under shear flow common to type III and IV flows, microlaminations develop where fine-grained silt layers alternate with sand and fine-gravel. These laminations may form as a result of multiple small scale depositional events or from grading within the flow.

Consistent with the laminar flow throughout the debris, little internal deformation of flow and underlying sediment is apparent in thin section. In contrast

with the larger folds in the dry-type flow deposits, small scale (<2mm) laminar undulations are present in wet-type flow deposits where the flow overrode an irregular surface or encountered a friction zone of a lag gravel. Similar to type I and II flows, pore fluid expulsion channels are often present in type III and IV flow deposits.

Type III and IV flows develop a better defined clast fabric, often omnisepic, than type I and II flows. In the Matanuska Glacier debris flow deposits, this clast fabric is most obvious in the apparent C-axes of phyllite clasts. In one sample (13) imbrication of phyllite clasts was well developed, a characteristic of type III flows deposited as fans (Lawson, 1979).

In contrast with type I and II flows, type III and IV flows often develop smooth décollement surfaces above their basal traction gravel. This surface is characterized by a planar zone of shear, often associated with an accumulation of finer grained material and silt in the lee of some gravels. Haloes are generally thin or nonexistent in wetter flows, which have less cohesion than dry-type flows.

Table 3. Micromorphological characteristics of subaerial glacigenic debris flow deposits

	DRY-TYPE	WET-TYPE
VISCOSITY	brittle to plastic deformation	plastic to laminar
REGIME AND	folding from compressive flow	thin flow laminations
STRUCTURES		décollement surfaces
CLAST FABRIC	often chaotic	omnisepic, often strongly
	sometimes lattisepic	developed
	often skelsepic	clasts may be imbricated upslope
		skelsepic common
FLOW/	underlying sediment deformation	little underlying sediment
SUBSTRATE	folding and faulting	deformation
INTERFACE		smooth contacts
FLUID	fluid escape structures	fluid escape structures
MOVEMENT	fluid injection structures	fluid injection structures
STRUCTURES		
HALOES	thick haloes	thin or nonexistent haloes

Ice marginal settings and debris flow deposits

Lawson observed that debris flows accounted for the majority of sediment deposition at the terminus of the Matanuska glacier (1979, 1982). Debris flow formation at the Matanuska Glacier is partly dependent on melting of debris-rich basal ice. The formation of debris-rich basal ice by freeze-on occurs in overdeepenings where supercooled water is expelled upward and downglacier, where it forms frazil ice as the pressure melting point is increased. The mesh-like frazil ice incorporates sediment during nucleation and eventually becomes a dense mass, which is transported subglacially and eventually exposed and ablated at the terminus (Strasser et al., 1996). If this situation is analogous to depositional settings of Pleistocene ice sheets in some locations, the presence of large amounts of subaerial debris flow deposits in ice marginal sediments of northern latitudes may indicate conditions of overdeepening and debris-rich basal ice formation. The Great Lakes basins and the Finger Lakes of western New York state may have supported conditions of overdeepening. The relationship between debris flows and debrisrich basal ice formation must be considered cautiously however; if the glacier or ice sheet is wet enough, substantial reworking of superglacial material and ablation of englacial debris bands may also permit debris flow formation (Boulton, 1968).

It should be noted, however, that the geologic situation at the Matanuska Glacier may be unique, and therefore may not serve as an analog for other glaciated locations. The Matanuska Glacier's sediment load is characterized by a large percentage of silt and sand, with only a small percentage of clay-sized particles (Lawson, 1979, 1982). The Laurentide

Ice Sheet of North America, on the other hand, often produced clay-rich sediments, which may have behaved differently than the silt-sized sediments at the Matanuska Glacier.

CONCLUSIONS

From the results presented in this paper, several conclusions can be reached: 1) Micromorphology can be used to distinguish wet from dry-types of debris flow deposits occurring at the Matanuska Glacier, Alaska. 2) The characteristic microstructures present in thin sections of debris flow deposits were often not visible in the field. 3) Dry-type debris flow deposits are characterized by a lack of a well defined clast fabric, generally exhibiting no clast fabric or a lattisepic and/or a skelsepic clast fabric, in addition to plastic and brittle deformation structures of the flow body and underlying sediments. Wet-type debris flow deposits are characterized by laminar flow structures, such as omnisepic clast fabrics, thin laminations, and a lack of underlying sediment deformation. 4) These microstructures are consistent with the physics and flow rheology occurring during transport and deposition of debris. 5) Laminar flow structures may be unique to wet-type debris flow deposits. In a glacial environment, while plastic and brittle microstructures in sediments may be polygenetic and postdepositional (van der Meer, 1993; Menzies, 1990), flow structures are generally only formed when a sediment source becomes saturated and flows under the influence of gravity. At a glacier's base, it is theoretically possible to develop structures having laminar characteristics. However, evidence of the subglacial conditions in a deforming bed (van der Meer, 1993; Menzies, 1990) indicate that brittle

and plastic structures rather than laminar structures dominate. Additionally, 6)
micromorphological analysis of other unconsolidated sediments will improve our ability to
provide genetic interpretations, and help in reconstructing depositional sequences
associated with recent and Pleistocene ice margins.

LIST OF REFERENCES

- Bouma, A.H., 1969. Methods for the study of Sedimentary Structures. John Wiley and Sons, New York.
- Boulton, G.S., 1968. Flow tills and related deposits on some Vestspitsbergen glaciers. Journal of Glaciology, v. 7, no. 51, p. 391-412.
- Brewer, R., 1976. Fabric and mineral analyses of soils. Krieger, Huntingdon NY, 482 pp.
- Evenson, E.B., Dreimanis, A., Newsome, J.W. 1977., Subaquatic flow tills: a new interpretation for the genesis of some laminated till deposits. Boreas, v. 6, p. 115-133.
- Fredericia, J., 1993. Macropore and fracture flow in clayey till: can thin sections be used in hydrogeology? Paper presented at the Technical Workshop: Micromorphology of sediments, Amsterdam.
- Hampton, M.A., 1975. Competence of fine-grained debris flows. Journal of Sedimentary Petrology, v. 45, no. 4, p. 834-844.
- Hartshorn, J.H., 1958. Flowtill in Southeastern Massachusetts. Bulletin of the Geological Society of America, v. 69, p. 477-482.
- Lawson, D.E., 1979. Sedimentological analysis of the western terminus region of the Matanuska Glacier, Alaska. Cold Regions Research and Engineering Laboratory (CRREL) Rep. 79-9.
- Lawson, D.E., 1982. Mobilization, movement and deposition of active subaerial sediment flows, Matanuska Glacier, Alaska. Journal of Geology, v. 90, p. 279-300.
- Marcussen, L., 1973. Studies on flow till in Denmark. Boreas, v. 2, p. 213-231.
- Marcussen, I., 1975. Distinguishing between lodgement till and flow till in Weichselian

- deposits. Boreas, v. 4, p. 113-123.
- Menzies, J., 1990. Brecciated diamictons from Mohawk Bay, S. Ontario, Canada. Sedimentology, v. 37, p. 481-493.
- Menzies, J., Maltman, A.J., 1992. Microstructures in diamictons Evidence of subglacial bed conditions. Geomorphology, v. 6, p. 27-40.
- Strasser, J.C., Lawson, D.A., Larson, G.J., Evenson, E.B., Alley, R.B., 1996.

 Preliminary results of tritium analyses in basal ice, Matanuska Glacier, Alaska, U.S.A.: evidence for subglacial ice accretion. Annals of Glaciology, v. 22, p. 126-132.
- van der Meer, J.J.M., 1987. Micromorphology of glacial sediments as a tool in distinguishing genetic varieties of till. Geological Survey of Finland, Special paper 3: 77-89.
- van der Meer, J.J.M., Laban, C., 1990. Micromorphology of some North Sea till samples, a pilot study. Journal of Quaternary Science, v. 5, p. 95-101.
- van der Meer, J.J.M., 1993. Microscopic evidence of subglacial deformation. Quaternary Science Reviews, v. 12, p. 553-587.

